

Optimization of Melanoma Skin Cancer Detection through Data Magnification, Filter Preprocessing, Image Enhancement, and Convolutional Techniques

Fatimah Asmita Rani¹

¹Multimatics, Indonesia

MEDINFTEch is licensed under a Creative Commons 4.0 International License.



ARTICLE HISTORY

Received: 12 July 2024
Final Revision: 15 July 25
Accepted: 12 August 25
Online Publication: 30 September 25

KEYWORDS

Convolution, Data Magnification, Image Enhancement, Melanoma, Skin Cancer Detection,

CORRESPONDING AUTHOR

Asmitarani1998@gmail.com

DOI

10.37034/medinftech.v3i3.48

A B S T R A C T

Melanoma skin cancer is one of the most aggressive forms of cancer, requiring early detection to improve patient outcomes. This study evaluates three image processing methods—Laplacian, Box Blur, and Edge Detection—used in melanoma detection, analyzing their performance using Mean Squared Error (MSE) and Structural Similarity Index (SSIM) metrics. Among these, Box Blur demonstrated the best overall performance with the lowest average MSE (104.16), indicating minimal distortion in the processed images. Additionally, it achieved the highest SSIM score (0.851), suggesting that it best preserved the structural integrity of the images, making it the most effective in maintaining both quality and important diagnostic details. In contrast, Edge Detection produced the highest MSE (108.02) and a negative SSIM score (-0.016), significantly distorting image structure and making it less suitable for melanoma detection. Laplacian, while moderate in performance, did not outperform Box Blur, with an MSE of 106.99 and an SSIM of 0.175. These results highlight Box Blur as the most reliable technique for melanoma image analysis, ensuring both clarity and structural preservation. By effectively enhancing diagnostic features and reducing errors, Box Blur offers a valuable tool for clinicians aiming to improve diagnostic accuracy in melanoma detection.

1. Introduction

Skin cancer is one of the most common types of cancer this decade. Considering that the skin is the largest organ in the human body, it is natural for skin cancer to be the most frequent type of cancer among humans [1]. Skin cancer is generally classified into two main categories: melanoma and nonmelanoma skin cancer [2]. Melanoma is a dangerous, rare, and deadly form of skin cancer. According to the American Cancer Society, melanoma accounts for only 1% of skin cancer cases but is responsible for a higher mortality rate. This occurs because melanoma develops in melanocytes, where genetic mutations or unrepaired DNA damage cause these cells to grow uncontrollably [3], [4]. Early detection is crucial for effective treatment, given its high mortality rate if not identified promptly. Nonmelanoma skin cancer (NMSC) is the most common type of cancer in the Western world, affecting primarily older adults but increasingly younger populations. Basal cell carcinoma (BCC) represents the majority of NMSC

cases, often appearing on the head and neck. To improve cosmetic outcomes, noninvasive diagnostic and monitoring techniques have been developed, aiming to reduce the need for invasive procedures [5], [6]. The development of these techniques marks a significant improvement in patient care, especially considering the rising demand for more effective and less intrusive diagnostic tools.

In comparison, melanoma is the deadliest type of skin cancer, responsible for approximately 55,500 deaths annually, or 0.7% of all cancer deaths worldwide. The incidence and mortality rates of melanoma vary by country, with differences attributed to ethnic and racial groups [7]. Melanoma cases are associated with a range of physical symptoms, such as dark lesions that may appear pink, white, or brown in some cases. Moreover, the texture and structure of melanoma lesions distinguish them from benign ones, highlighting the need for early and accurate detection [8]. The increasing incidence of melanoma and its potentially fatal

outcomes have driven significant advancements in early detection methods. Studies have focused on identifying melanoma in its earliest stages to improve patient survival rates. Recently, researchers have explored various techniques, including data augmentation and machine learning, to enhance detection accuracy. Esteva et al. (2021) demonstrated that data augmentation, such as image enlargement, improved the performance of a convolutional neural network (CNN) by increasing the diversity of the training dataset. This process involved rotating, flipping, scaling, and cropping images to simulate variations in skin lesion appearance. The results revealed that models trained with augmented datasets showed higher accuracy and sensitivity compared to those trained with original datasets alone, underscoring the significance of data augmentation in the medical domain.

Further advancements in preprocessing techniques, such as MinMax normalization, have also proven beneficial. Han et al. (2021) found that applying MinMax normalization before feeding skin lesion data into a CNN resulted in improved model convergence and classification accuracy. By scaling pixel values to the range [0, 1], MinMax normalization aids in stabilizing model learning, making it a valuable step in preprocessing for skin cancer detection models [9]. Despite the effectiveness of data augmentation and normalization techniques, more sophisticated tools have emerged for detecting skin cancer. One promising innovation is millimeter-wave radar, capable of distinguishing melanoma from healthy tissue by detecting variations in electrical properties. Homa Arab et al. developed a radar system operating at 77 GHz for biomedical imaging and skin cancer detection. This system is designed for high accuracy and cost efficiency, providing a less invasive method to detect melanoma in early stages, further emphasizing the need for diverse diagnostic tools [10].

In terms of computational approaches, both machine learning (ML) and deep learning (DL) have been employed to improve skin lesion classification accuracy. Youssef Filali et al. proposed a hybrid approach combining handcrafted features such as shape, color, and texture with deep learning features from CNNs. This combination addressed the limitations of each method, demonstrating promising results on both large and small datasets [11]. Similarly, research by Chandran Kaushik Viknesh et al. explored CNNs and support vector machines (SVMs) for melanoma classification. Their CNN-based method achieved higher accuracy, and the system was integrated into web and mobile applications for real-time melanoma detection [12].

The primary aim of this study is to develop an improved melanoma detection method by integrating techniques such as data augmentation, preprocessing enhancements, and convolutional neural networks. By building on the successes and addressing the limitations

of previous methods, this research seeks to provide a more accurate and efficient detection system for melanoma skin cancer. The study aims to compare the performance of the proposed techniques against existing approaches, focusing on their ability to handle diverse and complex datasets while maintaining high detection accuracy. Ultimately, by combining multiple techniques such as data augmentation, advanced preprocessing (e.g., MinMax normalization), and sophisticated detection tools like millimeter-wave radar this study intends to overcome the challenges of existing methods. It aims to create a more robust system that not only improves melanoma detection accuracy but also addresses issues related to dataset diversity, processing time, and real-time applications. This research seeks to contribute valuable insights into the future of computer-aided melanoma detection.

2. Research Method

The presented approach consists of four stages, namely: Starting with image enlargement using the LANCZOS resampling method which gives smooth results, the image is then subjected to processing with a MIN-MAX filter to reduce noise without losing the main structure of the image. The next step is contrasting enhancement using ImageEnhance, which clarifies the difference between light and dark areas to bring out important details. Then, various convolution filters are applied: Laplacian for fine edge detection, Box Blur for uniform smoothing, and Edge Detection to emphasize the boundaries of objects with high intensity. Figure 1 explains the proposed approach.

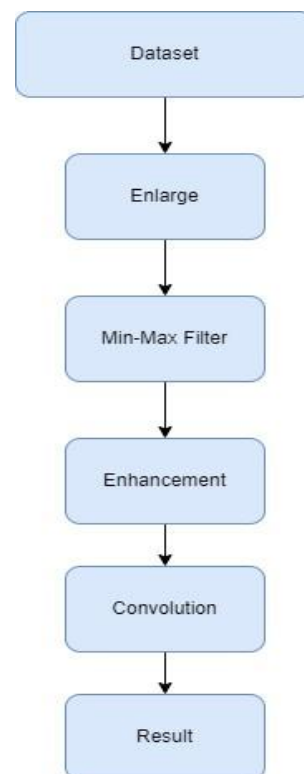


Figure 1. Process of The Proposed Method

2.1. Dataset

The melanoma dataset used in this study consists of images of skin lesions, specifically curated for research and development of skin cancer detection models, with a focus on melanoma. The dataset includes various types of lesions categorized as benign, malignant, or normal, and is accompanied by detailed annotations describing the characteristics of each image, such as texture, color, and lesion boundaries [13].

The dataset was obtained from publicly available sources, with a particular focus on datasets that have been widely used in skin cancer research. Prior to analysis, initial preprocessing steps were conducted to ensure data quality. These preprocessing steps included resizing the images for uniformity, applying contrast enhancement techniques to improve visibility of important features, and removing any duplicate or low-quality images to maintain consistency. Additionally, data augmentation methods, such as rotation and flipping, were used to increase the variability in the dataset and prevent overfitting during model training.

To ensure high data quality, the images were carefully inspected to verify that the annotations were accurate and consistent with clinical standards. This meticulous curation process helps ensure the reliability of the dataset, directly influencing the accuracy and performance of the machine learning and deep learning models developed. For this study, 40 melanoma skin cancer datasets were selected. Figure 2 shows an image of a benign melanoma, and Figure 3 illustrates a malignant melanoma.

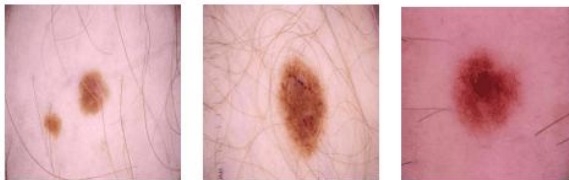


Figure 2. Benign Cancer



Figure 3. Malignant Cancer

2.2. Enlarge

The Lanczos method is an image enhancement technique used to enlarge images while maintaining high visual quality. This technique uses a Lanczos kernel, which is a truncated sinc function, to calculate new pixel values in the enlarged image. The Lanczos process involves using the coefficients of this kernel to weight the contributions of several pixels around each

enlarged pixel, thus producing a smoother and more detailed image by reducing artifacts such as aliasing. The value of each new pixel is calculated as a weighted sum of the surrounding pixels, with the weights determined by the Lanczos kernel, which ensures that the contribution from more distant pixels is reduced. This method is more complex and requires more calculations than simple interpolation methods such as bilinear or bicubic, but is capable of producing smoother images and retaining more visual detail [14].

Below is the formula (1) for the lanczos method:

$$A_y = AV_x = VTV * V_x = VTl_x = VT_x = V(\lambda x) = \lambda V_x = \lambda_y \quad (1)$$

Where, A is the matrix being approximated, and V_x represents a vector from the orthogonal basis V generated during the Lanczos iterations. The product AV_x results in a new vector A_y , which represents the transformation of the original matrix A by the vector V_x . The term VTV represents the matrix A being decomposed into a tridiagonal matrix T using the orthogonal basis vectors in V, allowing for efficient computations.

The variable λ is an eigenvalue of the matrix T, and it scales the vector V_x , yielding λV_x . This step approximates how the matrix A acts on its eigenvectors, enabling the identification of the eigenvalues of A through the smaller matrix T. By following this process, the Lanczos method reduces the computational complexity associated with large matrices while preserving the key characteristics necessary for eigenvalue calculations or solving linear systems.

2.3. Filter MIN-MAX

The MIN-MAX filter in image processing is a non-linear technique used to smooth images and reduce noise by replacing the pixel value at the center of the filter window with the minimum or maximum value of the surrounding pixels in the window. The Minimum Filter (Min Filter) replaces the center pixel value with the minimum pixel value within the window, which is effective for removing impulse noise or "salt noise". Conversely, the Maximum Filter (Max Filter) replaces the center pixel value with the maximum pixel value within the window, which is effective for removing impulse noise or "pepper noise" [15]. This technique is simple and easy to implement, and is effective in reducing impulse noise, but can cause loss of image detail, especially on edges and fine lines. The use of MIN-MAX filters is essential in image processing to remove certain types of noise in an efficient manner [16].

Below is the formula of the MIN-MAX filter [17].

$$x_t = \frac{\min(x_i+d_i)+\max(x_i-d_i)}{2} \quad (2)$$

$$y_t = \frac{\min(y_i + d_i) + \max(y_i - d_i)}{2} \quad (2)$$

Where, x_i and y_i represent the pixel intensities in the x - and y - coordinates at position i . d_i is a small adjustment value or neighborhood size that determines how far to look for the minimum and maximum values in the surrounding pixels. $\min(x_i + d_i)$ and $\max(x_i - d_i)$ are the minimum and maximum values computed within a local neighborhood around the pixel.

The goal of this filter is to calculate the average of the local minimum and maximum pixel values within a defined neighborhood. This averaging helps to smooth out noise by reducing the impact of extreme values (such as noise spikes) while maintaining the overall structure of the image. By applying the MIN-MAX filter in both x - and y -directions, the image becomes cleaner, with less noise and fewer artifacts, but still retains important edges and details.

This filter is particularly useful where noise needs to be reduced without significant blurring, which is essential for preserving edges and fine details in the image.

2.4. Enhancement

Contrast enhancement in image processing is a technique used to increase the difference between the intensities of adjacent pixels in an image. One commonly used method is Histogram Equalization, where the intensity distribution of pixels across a range of intensity values is altered to flatten the image histogram. This technique is effective in enhancing details hidden in shadows or highlights, resulting in a sharper and more visually dynamic image [18], [19]. In addition, Contrast Stretching is also often used, where the range of pixel intensities is extended from the minimum to the maximum value present in the image, increasing the overall contrast. These two methods can be applied in various ways to improve image quality in a wide range of applications, from medical analysis to object recognition in computer vision [20].

Here is the formula (3) for histogram equalization [21].

$$I_{\text{equalized}}(x, y) = \left\lfloor \frac{(L-1)}{(M \times N)} \sum_{i=0}^{I(x,y)} H(i) \right\rfloor \quad (3)$$

Where, $I_{\text{equalized}}(x, y)$ is the new pixel intensity, $I(x, y)$ the original intensity at coordinates $H(i)$ a histogram that stores the number of pixels, L the number of intensity levels, and M, N the image dimensions [21].

2.5. Convolution

In image processing, Laplacian convolution filters are often used to detect smooth edges [22]. This filter works by identifying sharp changes in pixel intensity around a particular point in the image. This makes it possible to find edges that are not too rough or sharp, helping in analyses that require finer and more detailed edge detection [23].

Meanwhile, the Box Blur filter is one of the techniques for uniform smoothing or reducing noise in an image [24]. This filter works by flattening the pixel values around each point in the image, producing a smoothing effect and reducing sharp variations between neighboring pixels. This is useful for removing small details or unwanted noise from the image, improving overall visual clarity.

In addition, edge detection techniques in image processing, such as using Sobel or Canny filters, focus on identifying drastic changes in pixel intensity, which signify boundaries between objects or features in the image [25]. These techniques are used for object segmentation, pattern recognition, and many other applications that require a detailed understanding of the image structure.

The application of such convolutional filter combinations can improve image processing by optimizing edge detection, reducing noise, and sharpening relevant details according to specific application needs.

In general, the image convolution formula is as follows:

$$I(x, y) = \sum_i \sum_j I(x - i, y - j) \cdot K(i, j) \quad (4)$$

Where I is the original image, K is the kernel, (i, j) is the index of the kernel and (x, y) is the pixel coordinate in the image.

2.6. Mean Squared Error (MSE)

Mean Squared Error (MSE) is a widely used metric for evaluating the performance of regression models [26]. It is calculated by taking the average of the squared differences between the predicted values and the actual values, as shown by the formula:

$$MSE = \frac{1}{m} \sum_{i=1}^m (X_i - Y_i)^2 \quad (5)$$

Where m is the number of data points, X_i represents the predicted value, and Y_i represents the true value. The best possible MSE is 0, indicating perfect predictions, while the worst value can theoretically be infinite [26].

One key feature of MSE is its sensitivity to outliers, due to the squaring of errors. When there is a large deviation between a prediction and the true value, the squared error is magnified, making MSE particularly useful for detecting outliers. This property stems from the L2 norm, which amplifies larger errors more than smaller ones. Therefore, a single poor prediction can significantly impact the overall MSE score, which is beneficial when identifying problematic data points but can also make MSE prone to being skewed by outliers.

In terms of methodology, MSE is advantageous when it is important to give more weight to large errors, especially in cases where the model's performance on extreme values is critical. However, this sensitivity can also be a limitation if the model is overly penalized for

outliers, making MSE less ideal when outliers are not a concern. Therefore, while MSE is useful for identifying large errors, it may be complemented by other metrics, such as Mean Absolute Error (MAE), to provide a more balanced evaluation of model performance.

2.7. Structural Similarity Index (SSIM)

The Structural Similarity Index (SSIM) is a widely used metric for measuring the similarity between two images, focusing on perceived changes in structural information. The methodology for calculating SSIM involves several key steps [27], [28].

First, the two images to be compared, typically the original image I and the processed image P , are converted to grayscale if they are in color, as SSIM primarily assesses luminance [28]. Next, the images are divided into small overlapping windows (or patches) of size $N \times N$. For each window, the SSIM index is computed based on three components: luminance, contrast, and structure.

The luminance component quantifies the brightness similarity between the two images, calculated as:

$$L(x, y) = \frac{2\mu_I\mu_P + C_1}{\mu_I^2 + \mu_P^2 + C_1} \quad (6)$$

Where μ_I and μ_P are the mean pixel values of the windows in the original and processed images, respectively, and C_1 is a small constant to prevent division by zero [27], [28].

The contrast component assesses the variability (or contrast) of the images, calculated as:

$$C(x, y) = \frac{2\sigma_I\sigma_P + C_2}{\sigma_I^2 + \sigma_P^2 + C_2} \quad (7)$$

Where σ_I and σ_P are the standard deviations of the pixel values in the respective windows, and C_2 is another small constant [27], [28].

The structure component measures the correlation between the two images, defined as:

$$S(x, y) = \frac{\sigma_{IP} + C_3}{\sigma_I\sigma_P + C_3} \quad (8)$$

Where σ_{IP} is the covariance of the pixel values between the two windows, and C_3 is a small constant.

Finally, the overall SSIM index for the two images is calculated by combining these three components:

$$SSIM(x, y) = L(x, y) \cdot C(x, y) \cdot S(x, y) \quad (9)$$

Where, the SSIM value ranges from -1 to 1, with 1 indicating perfect structural similarity, 0 representing no similarity, and negative values indicating significant distortion or differences [27], [28].

By averaging the SSIM values of all windows, a single SSIM score for the entire image pair is obtained, providing a comprehensive assessment of the perceived quality and structural integrity of the processed image

compared to the original. This method is particularly valuable in applications such as medical imaging, where maintaining structural fidelity is crucial for accurate diagnosis and analysis.

3. Result and Discussion

The results of applying the enlarge method, MIN-MAX filter pre-processing, enhancement and convolution using a dataset of 40 melanoma skin cancer image data. The process begins with image enlargement using the LANCZOS resampling method, then the image undergoes processing with the MIN-MAX filter. The next step is contrasting enhancement using ImageEnhance, and applying Laplacian convolution filter, Box Blur for uniform smoothing, and Edge Detection. The outcomes of these stages are summarised in Table 1.

Table 1. Result the Image

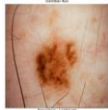
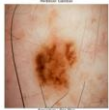
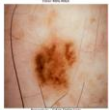
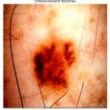
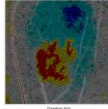
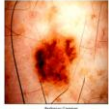
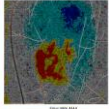
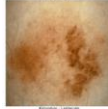
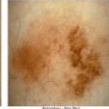
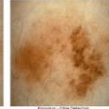
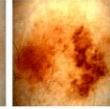
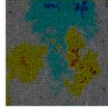
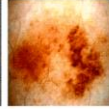
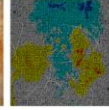


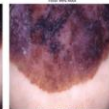
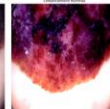
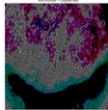

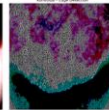

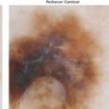
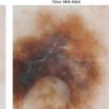

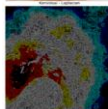
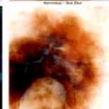
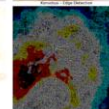
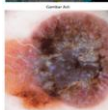

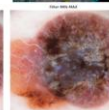
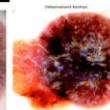
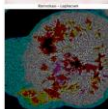

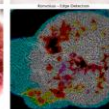
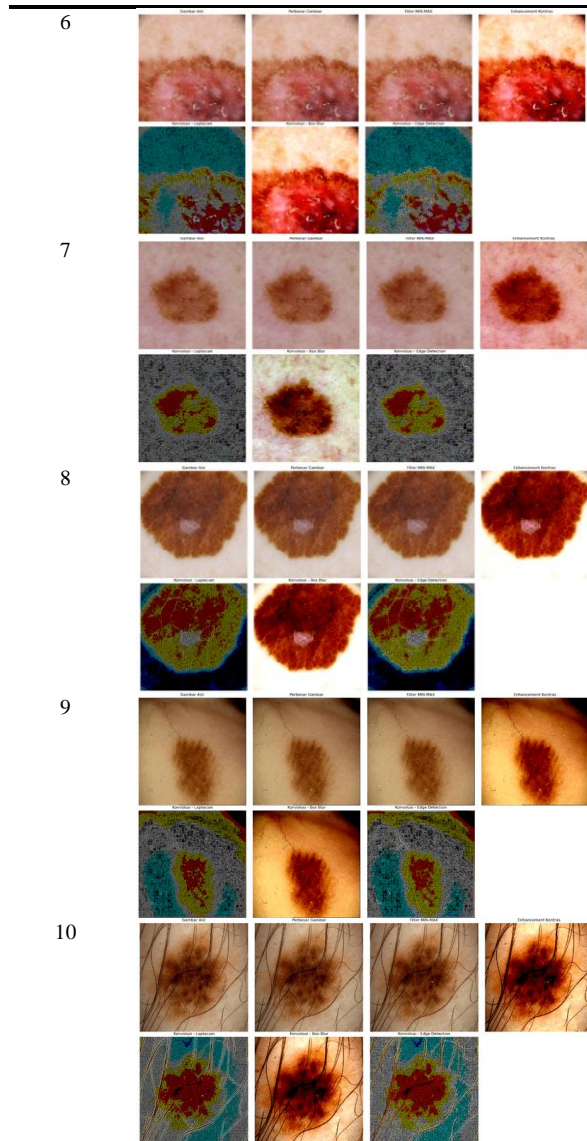
Figure	Result			
1				
				
2				
				
3				
				
4				
				
5				
				

Table 2. Result the Image (Continue)



Below is the table showing the accuracy results for 40 images using Mean Squared Error (MSE) and Structural Similarity Index (SSIM), as summarized in Table 2.

Table 2. Result of Accuracy from MSE and SSIM

	MSE	SSIM
Laplacian	106.990	0.175
Box Blur	104.160	0.851
Edge Detection	108.020	-0.016

Based on the evaluation results from processing 40 melanoma images, clear differences emerge between the performance of the Laplacian, Box Blur, and Edge Detection methods. The assessment was conducted using two key metrics: Mean Squared Error (MSE) and the Structural Similarity Index (SSIM).

MSE measures the average squared error between the original and processed images, where a lower MSE indicates better performance. From the average results, Box Blur demonstrated the lowest MSE, with a value of

104.16, indicating that this method introduced the least distortion to the images compared to the others. On the other hand, Edge Detection had the highest MSE, at 108.02, suggesting that this method resulted in greater errors when detecting edges in the images.

In terms of SSIM, which evaluates the structural similarity between the original and processed images, Box Blur again proved to be the most effective, with the highest SSIM value of 0.851, indicating that it was the best at preserving the structural integrity of the images. Edge Detection, however, showed a negative SSIM score of -0.016, meaning it significantly distorted the structure of the images. Laplacian performed moderately well, with an SSIM score of 0.175, though still far below the performance of Box Blur.

Overall, these results indicate that Box Blur is the most effective method for preserving image quality and structural integrity, making it the optimal choice for image processing, especially in the analysis of melanoma images where precision is crucial. Laplacian performed moderately, while Edge Detection proved to be less effective in preserving both quality and structure, making it unsuitable for applications that require high accuracy. If the main goal is to maintain image quality and reduce noise without losing important details, Box Blur stands out as the best option.

4. Conclusion

In conclusion, the evaluation of various image processing techniques on a dataset of 40 melanoma skin cancer images highlights the effectiveness of the Box Blur method in preserving image quality. The results, demonstrated through both Mean Squared Error (MSE) and Structural Similarity Index (SSIM) analyses, reveal that Box Blur consistently achieved the lowest MSE values, indicating minimal loss of original image quality, along with the highest SSIM scores that reflect its superior perceptual similarity to the original images. Conversely, the Laplacian and Edge Detection methods exhibited higher MSE and lower SSIM values, suggesting a tendency to distort the images and compromise structural integrity.

These findings have significant implications for real medical practice, particularly in the diagnosis and treatment of skin cancer. By utilizing the Box Blur technique, dermatologists and medical professionals can enhance the clarity and detail of melanoma images, leading to more accurate assessments and improved visualization of critical features that inform treatment decisions. Enhanced image quality may facilitate better pattern recognition and identification of malignant lesions, ultimately aiding in early detection and timely intervention.

For further research, it would be valuable to explore the integration of advanced techniques such as deep learning-based image processing, which have shown promise in medical imaging. Additionally, investigating

hybrid methods that combine the strengths of Box Blur with other techniques, such as adaptive filtering or machine learning algorithms, could further improve the robustness and accuracy of melanoma image enhancement. Exploring real-time processing capabilities would also enhance clinical workflows, enabling immediate analysis during patient examinations. These avenues for future research could lead to significant advancements in medical image processing and improve outcomes in skin cancer diagnosis and treatment.

References

- [1] P. Aggarwal, P. Knabel, and A. B. Fleischer, "United States burden of melanoma and non-melanoma skin cancer from 1990 to 2019," *J. Am. Acad. Dermatol.*, vol. 85, no. 2, pp. 388–395, 2021, doi: 10.1016/j.jaad.2021.03.109.
- [2] H. Bhatt, V. Shah, K. Shah, R. Shah, and M. Shah, "State-of-the-art machine learning techniques for melanoma skin cancer detection and classification: a comprehensive review," *Intell. Med.*, vol. 3, no. 3, pp. 180–190, 2023, doi: 10.1016/j.imed.2022.08.004.
- [3] M. Dildar *et al.*, "Skin cancer detection: A review using deep learning techniques," *Int. J. Environ. Res. Public Health*, vol. 18, no. 10, 2021, doi: 10.3390/ijerph18105479.
- [4] M. H. Trager, L. J. Geskin, F. H. Samie, and L. Liu, "Biomarkers in melanoma and non-melanoma skin cancer prevention and risk stratification," *Exp. Dermatol.*, vol. 31, no. 1, pp. 4–12, 2022, doi: 10.1111/exd.14114.
- [5] H. D. Heibel, L. Hooey, and C. J. Cockerell, "A Review of Noninvasive Techniques for Skin Cancer Detection in Dermatology," *Am. J. Clin. Dermatol.*, vol. 21, no. 4, pp. 513–524, 2020, doi: 10.1007/s40257-020-00517-z.
- [6] M. Hyeraci *et al.*, "Systemic Photoprotection in Melanoma and Non-Melanoma Skin Cancer," *Biomolecules*, vol. 13, no. 7, pp. 1–14, 2023, doi: 10.3390/biom13071067.
- [7] J. Daghrir, L. Tlig, M. Bouchouicha, and M. Sayadi, "Melanoma skin cancer detection using deep learning and classical machine learning techniques: A hybrid approach," *2020 Int. Conf. Adv. Technol. Signal Image Process. ATSIP 2020*, no. C, pp. 1–5, 2020, doi: 10.1109/ATSIP49331.2020.9231544.
- [8] M. Shorfuzzaman, "An explainable stacked ensemble of deep learning models for improved melanoma skin cancer detection," *Multimed. Syst.*, vol. 28, no. 4, pp. 1309–1323, 2022, doi: 10.1007/s00530-021-00787-5.
- [9] M. Oumoulyte, A. O. Alaoui, Y. Farhaoui, A. El Allaoui, and A. Bahri, "Convolutional neural network-based approach for skin lesion classification," *Data Metadata*, vol. 2, 2023, doi: 10.56294/dm2023171.
- [10] H. Arab, L. Chioukh, M. Dashti Ardakani, S. Dufour, and S. O. Tatu, "Early-Stage Detection of Melanoma Skin Cancer Using Contactless Millimeter-Wave Sensors," *IEEE Sens. J.*, vol. 20, no. 13, pp. 7310–7317, 2020, doi: 10.1109/JSEN.2020.2969414.
- [11] Y. Filali, H. EL Khoukhi, M. A. Sabri, and A. Aarab, "Efficient fusion of handcrafted and pre-trained CNNs features to classify melanoma skin cancer," *Multimed. Tools Appl.*, vol. 79, no. 41–42, pp. 31219–31238, 2020, doi: 10.1007/s11042-020-09637-4.
- [12] C. K. Viknesh, P. N. Kumar, R. Seetharaman, and D. Anitha, "Detection and Classification of Melanoma Skin Cancer Using Image Processing Technique," *Diagnostics*, vol. 13, no. 21, 2023, doi: 10.3390/diagnostics13213313.
- [13] S. Gupta, J. R. A. K. Verma, A. K. Saxena, A. K. Moharana, and S. Goswami, "Ensemble optimization algorithm for the prediction of melanoma skin cancer," *Meas. Sensors*, vol. 29, no. July, p. 100887, 2023, doi: 10.1016/j.measen.2023.100887.
- [14] H. Kim, S. M. Choi, C. S. Kim, and Y. J. Koh, "Representative Color Transform for Image Enhancement," *Proc. IEEE Int. Conf. Comput. Vis.*, pp. 4439–4448, 2021, doi: 10.1109/ICCV48922.2021.00442.
- [15] R. A. Khamis, M. O. Shafiq, and A. Matrawy, "Investigating Resistance of Deep Learning-based IDS against Adversaries using min-max Optimization," *IEEE Int. Conf. Commun.*, vol. 2020-June, 2020, doi: 10.1109/ICC40277.2020.9149117.
- [16] P. Satti, N. Sharma, and B. Garg, "Min-Max Average Pooling Based Filter for Impulse Noise Removal," *IEEE Signal Process. Lett.*, vol. 27, no. April 2021, pp. 1475–1479, 2020, doi: 10.1109/LSP.2020.3016868.
- [17] K. Yang, Z. Liang, R. Liu, and W. Li, "RSS-Based Indoor Localization Using Min-Max Algorithm with Area Partition Strategy," *IEEE Access*, vol. 9, pp. 125561–125568, 2021, doi: 10.1109/ACCESS.2021.3111650.
- [18] K. G. Dhal, A. Das, S. Ray, J. Gálvez, and S. Das, "Histogram Equalization Variants as Optimization Problems: A Review," *Arch. Comput. Methods Eng.*, vol. 28, no. 3, pp. 1471–1496, 2021, doi: 10.1007/s11831-020-09425-1.
- [19] B. S. Rao, "Dynamic Histogram Equalization for contrast enhancement for digital images," *Appl. Soft Comput. J.*, vol. 89, p. 106114, 2020, doi: 10.1016/j.asoc.2020.106114.
- [20] X. Li, L. Yu, H. Chen, C. W. Fu, L. Xing, and P. A. Heng, "Transformation-Consistent Self-Ensembling Model for Semisupervised Medical Image Segmentation," *IEEE Trans. Neural Networks Learn. Syst.*, vol. 32, no. 2, pp. 523–534, 2021, doi: 10.1109/TNNLS.2020.2995319.
- [21] Y. Li *et al.*, "A novel detail weighted histogram equalization method for brightness preserving image enhancement based on partial statistic and global mapping model," *IET Image Process.*, vol. 16, no. 12, pp. 3325–3341, 2022, doi: 10.1049/ipr2.12567.
- [22] R. Haryono, "Penerapan Metode Laplacian Of Gaussian Dalam Mendeteksi Tepi Citra Pada Penyakit Meningitis," *KLIK (Kajian Ilm. Inform. Komputer)*, vol. 1, no. 1, pp. 20–26, 2020, [Online]. Available: <https://djournals.com/klik/article/view/21/5>
- [23] M. Sayed and G. Brostow, "Improved Handling of Motion Blur in Online Object Detection," *Proc. IEEE Comput. Soc. Conf. Comput. Vis. Pattern Recognit.*, no. 4, pp. 1706–1716, 2021, doi: 10.1109/CVPR46437.2021.00175.
- [24] W. Zhao, C. Shang, and H. Lu, "Self-generated Defocus Blur Detection via Dual Adversarial Discriminators," *Proc. IEEE Comput. Soc. Conf. Comput. Vis. Pattern Recognit.*, pp. 6929–6938, 2021, doi: 10.1109/CVPR46437.2021.00686.
- [25] D. Sharifrazi *et al.*, "Fusion of convolution neural network, support vector machine and Sobel filter for accurate detection of COVID-19 patients using X-ray images," *Biomed. Signal Process. Control*, vol. 68, no. April, p. 102622, 2021, doi: 10.1016/j.bspc.2021.102622.
- [26] D. Chicco, M. J. Warrens, and G. Jurman, "The coefficient of determination R-squared is more informative than SMAPE, MAE, MAPE, MSE and RMSE in regression analysis evaluation," *PeerJ Comput. Sci.*, vol. 7, pp. 1–24, 2021, doi: 10.7717/PEERJ-CS.623.
- [27] V. Mudeng, M. Kim, and S. W. Choe, "Prospects of Structural Similarity Index for Medical Image Analysis," *Appl. Sci.*, vol. 12, no. 8, 2022, doi: 10.3390/app12083754.

- [28] F. Osorio, R. Vallejos, W. Barraza, S. M. Ojeda, and M. A. Landi, “Statistical estimation of the structural similarity index for image quality assessment,” *Signal, Image Video Process.*, vol. 16, no. 4, pp. 1035–1042, 2022, doi: 10.1007/s11760-021-02051-9.